Molecular Motion and Transitions in Solid Tripalmitin Measured by Deuterium Nuclear Magnetic Resonance[1]

T.M. Eads*, A.E. Blaurock[2], R.G. Bryant[3], D.J. Roy[2] and W.R. Croasmun[2]
Department of Food Science and Whistler Center for Carbohydrate Research, Smith Hall, Purdue University, West Lafayette, Indiana 47907-1160

Deuterium nuclear magnetic resonance (NMR) quadrupole echo spectra of deuterated acyl chains and the glyceryl moiety of tripalmitin were found to depend on the crystal form. At 20°C, which is below melting points, line shapes indicate that molecular motions in the β form (triclinic subcell) are more restricted than in β' (orthorhombic) or α (hexagonal). Motional rates in excess of about 20 kHz are responsible for the line shapes. Spin-lattice relaxation, sensitive to motional frequencies in the tens of megahertz range, is much faster for methyl (CD_2) groups in α or β' than in β, indicating that fast motions are also governed by crystal form. General theoretical considerations suggest that motion of methylene groups is dynamically heterogeneous and that motion of methyl (CD_3) groups may be averaged by motions other than rotation about the terminal C-C bond. The isothermal solid-state transition from α to β, induced by increasing the temperature to 35°C, was accompanied by NMR lineshape changes consistent with immobilization. The reversible transition of α to "sub-α" upon cooling, accompanied by orthorhombic-like Bragg spacings and other changes in the X-ray pattern and by corresponding changes in the infrared spectrum, also produced a marked restriction in NMR-detected mobility of the kind seen in β' relative to α. The advantages of ^2H NMR for studies of motions and transitions in solid glycerides are discussed.

KEY WORDS: Deuterium NMR, infrared, molecular motion, phase transitions, polymorphism, solid fat, tripalmitin, X-ray diffraction.

Solid triacylglycerols (fats) play important roles in a range of phenomena in food texture and stability (1–3). A large number of triacylglycerol species occur naturally. In the variety of crystalline or liquid crystalline structures they may adopt, there are simplifying patterns because the crystalline lattices are dominated by interactions between the hydrocarbon tails of the acyl groups (4–6). The principal acyl chain subcell symmetries in triacylglycerols include the so-called α (hexagonal lattice), β' (orthorhombic) and β (triclinic) (7–9). The latter two may have several variants, classified according to their X-ray diffraction patterns and infrared spectra. It is well known that fundamental properties such as density, melting point, heat of fusion, rate of crystallization, rate of solid transitions and surface characteristics depend on crystal form, and some theoretical progress has been made toward predicting some of these properties for triacylglycerols (10–14). However, the mechanisms that connect arrangement and motions of glyceride molecules to complex properties such as mechanical response, texture, lubricity, surface chemical reactivity, permeability of crystalline domains to small molecules, *etc.*, are not well investigated and require both experimental and theoretical approaches.

For semicrystalline polymers, molecular motion in the solid state, determined primarily by nuclear magnetic resonance (NMR), has been related to functional properties. See, for example, Komoroski and Mandelkern (15). It is reasonable to expect similar relationships to hold for the glycerides. NMR approaches for analysis of lipids, particularly triglycerides, have been reviewed (16–19).

A major experimental challenge is to quantify the rates, amplitudes and orientations of molecular motions. Motion in solids is geometrically restricted, and the distribution of frequencies for such motions is different from that in liquids. The hypothesis that the triglyceride lattice with less restriction, namely the α (hexagonal) form, should permit large amplitude motions to occur has been tested by NMR. Using the continuous wave method, Chapman (20) measured wide-line ^1H NMR spectra of various glycerides and showed that at 293K, polymorphic form governs the line shape, and by inference, chain motions, with α being more mobile than β. This work indicated the fundamental similarity between the wide-line ^1H NMR behavior of glycerides and other acyl chain-containing compounds (21). Other workers have found that ^1H nuclear relaxation times depend on crystal form and temperature in ways useful for diagnosis of lattice mobility in mixed triglycerides (22,23) and triglyceride-emulsifier systems (24). ^{13}C NMR chemical shifts, at least of the glyceryl carbons (25), and ^1H spin-lattice relaxation times (23) are also sensitive to polymorphic form. The ^1H relaxation results confirmed Chapman's previous observation (20) of greater molecular flexibility in the less dense lattices, but the location of greater flexibility could not be specified.

Deuterium (^2H) NMR is well suited for observation of molecular motions in the solid state. Because the natural abundance of ^2H is low, it is usually necessary to replace hydrogen with deuterium at selected molecular sites. A well-developed theory exists for interpretation of ^2H NMR spectra in terms of rates and amplitudes of motions in specified molecular frames of reference. Extensive applications of ^2H NMR to membrane studies have been reviewed by Seelig (26), Griffin (27), Davis (28), Smith and Oldfield (29) and to polymer and liquid crystal studies by Spiess (30,31), Luz (32) and Samulski (33). Applications involving labelled triglycerides appear to be limited to one study of triglyceride mobilty in bilayer membranes (34). In the present work, we use deuterium solid-state NMR to measure molecular dynamics in three important crystalline forms of tripalmitin and to characterize the motional consequences of certain thermally induced structural transitions in the solid state. The relationships among lattice geometry, volume and mobility are discussed. Preliminary reports of this work have been presented (35–37).

EXPERIMENTAL PROCEDURES

Deuterium labeling. Glyceryl-deuterated tripalmitin, with ^2H replacing glycerol hydrogen atoms, was prepared from

[1]Presented at the 80th Annual Meeting of AOCS in Cincinnati, May 1989, and at the 81st Annual Meeting in Baltimore, May 1990.
*To whom correspondence should be addressed.
[2]Kraft General Foods, Inc., Technology Center, 801 Waukegan Rd., Glenview, IL 60025.
[3]Department of Biophysics, University of Rochester Medical Center, 601 Elmwood Ave., Rochester, NY 14642.

glycerol-d_5 and palmitic acid according to the method of Gorrisen *et al.*(34). Chain-deuterated tripalmitin, in which 56% of the fatty acid chains at the 1- and 3-position of the glycerol were substituted by palmitic acid-d_{31}, was prepared by enzymatic interesterification of tripalmitin with the deuterated fatty acid by means of *Mucor miehei* lipase (Lipase 3A, Novo Enzyme Co. Laboratories, Wilton, CT). The degree of substitution was estimated from the ratio of the starting materials, assuming an equilibrium reaction product and determined experimentally by NMR and high-resolution gas chromatography. Both synthetic products were purified by thin-layer chromatography and recovered by solvent evaporation. Sample identity and purity were confirmed by solution ^2H NMR (glyceryl-deuterated tripalmitin) or by a combination of ^1H and ^2H NMR (chain-deuterated tripalmitin). Percent exchange at the 1 and 3 chain positions in chain-deuterated tripalmitin was calculated to be 56% from integration of the ^1H NMR spectrum.

High-resolution gas chromatography. Deuterated tripalmitin samples were analyzed for chromatographable glyceride content on a 10-m capillary column coated with a nonpolar stationary phase. Prior to analysis, the samples were derivatized with N-methyl-N-*t*-butyl-dimethylsilyltrifluoroacetamide. The glyceride content of glyceryl-deuterated tripalmitin was found to be 98.22% triglyceride by this method, the remainder being monoglyceride. Similarly, the glyceride content of the chain-deuterated triglyceride was 99.61% triglyceride, the remainder being monoglyceride. For the chain-deuterated compound, three peaks were observed, corresponding to 33.03, 49.98, and 16.79% of total triglyceride material. These three peaks correspond to triglycerides with two labelled hydrocarbon chains, one labelled chain, and no labelled chain, respectively. Suppose x represents the fraction of chains at the 1- and 3-position that are labelled. The enzyme exchanges only at the 1- and 3-position, labelled chains are distributed randomly between the 1- and 3-site, and molecules labelled only at the 1-site or only at the 3-site are indistinguishable. Then, x^2 will be the fraction of doubly labelled triglycerides and $(1-x)^2$ will be the fraction of unlabelled triglycerides. Fraction x is estimated to be 0.57 from the observed fraction of triglycerides with two labelled chains or 0.59 from the observed fraction of unlabelled triglycerides. This agrees well with the NMR result.

Differential scanning calorimetry (DSC) methods. Both unlabelled tripalmitin and deuterated tripalmitin were characterized by their melting behavior with DSC (Perkin-Elmer DSC-7, Norwalk, CT). Specimens weighing a few milligrams were sealed in aluminum sample pans, heated to 100°C and then subjected to either of two temperature programs: (i) For isothermal crystallization, the specimen was cooled at 10°C/min down to the set temperature and then held there for crystallization to occur; (ii) Specimens were cooled at 10°C/min to −50°C and then heated at the same rate to melt the crystals formed during cooling. Typically, α crystals, formed during the cooling leg, melted at $T_\alpha = 45°C$ (6); this melt crystallized very quickly to β', which transformed gradually to β *via* a solid-solid transition. Finally, the β crystals melted at about 66°C [T_β; (6)]. Melting temperatures were the same for unlabelled and deuterated tripalmitin, and the same as published values for tripalmitin, to within 1–2°C. Heat of fusion of β tripalmitin, 190 J/g, was somewhat smaller than a published value, 212 J/g (6); in our experience, a decrement of this size can result because the newly formed β crystals have not been tempered for a sufficiently long time before melting.

Preparation of crystal forms. The different crystal forms were prepared by holding unlabelled or deuterated tripalmitin at 100°C for at least five minutes to ensure melting and then quenching to the prescribed temperature and holding for a carefully selected time. Temperatures and holding times for the respective forms were based on a DSC study of crystallization and solid-solid transitions in tripalmitin (Blaurock, A.E. and F.J. Sasevich, unpublished data).

To make α tripalmitin, the molten material was quenched by immersing the 5-mm NMR tube in water at 25°C. For β tripalmitin, α crystals were formed in this way, and then the specimen was heated to 60°C, to melt α and β' crystals; β crystals thus form spontaneously and rapidly. In one instance, β crystals were formed by holding the α crystals somewhat below T_α (45°C). To make β' crystals, the molten material was quenched at 46°C, *i.e.* just above T_α, and held for five minutes. These were then stabilized by quenching the specimen in water at 20°C. The so-called sub-α crystals were formed by cooling α crystals to temperatures well below 0°C. Crystal form was identified for the NMR specimen by X-ray diffraction as described below.

X-Ray diffraction methods. X-rays (predominantly Cu K_α, $\lambda = 1.542$ Å) were generated in a Rigaku microfocus rotating-anode generator with copper target. The diffraction camera was of the Franks type (38), with focusing glass flats that filter out short-wavelength white radiation. Specimens were placed in a chamber with thin Melinex windows, and the temperature was controlled by a thermostated, refrigerated circulating bath. For experiments at low temperatures, the specimen chamber was cooled by a flow of nitrogen gas obtained by boiling liquid nitrogen; the temperature was not thermostatically controlled, and it drifted by a few degrees during the 1–2 min required to record an X-ray pattern. Temperature was measured with a thermocouple (Omega Digital Data Logger, Omega Engineering, Stamford, CT). A position-sensitive X-ray detector (PSD) (M. Braun, West Germany; supplied by Innovative Technology, Inc., South Hamilton, MA) was used to record the diffraction pattern. The PSD chamber was pressurized with P-10 gas (90% argon, 10% methane) at about 6 bar. Diffraction patterns were accumulated in a multi-channel analyzer and then transferred to an IBM PC-AT for analysis.

Crystal form was determined both before and after the NMR experiment. A key point here is the use of the PSD. Because the 5-mm diameter NMR specimen was much thicker than the optimum (about 1 mm), and because the glass walls of the NMR tube absorb X-rays strongly, counting rates were of the order of 10 ct/s, which compares to a rate of a few thousand ct/s from an optimum X-ray specimen. Thus, exposures up to 1 h were required to record sufficient X-ray counts to detect reflections in the wide-angle region diagnostic of crystal form.

As shown in Figure 1, α crystals give a single, somewhat broadened diffraction peak; β' crystals give two peaks: β crystals give three major peaks; and sub-α crystals give a single, asymmetrically broadened peak. For each crystal form, the widths of peaks are a measure of crystallite size.

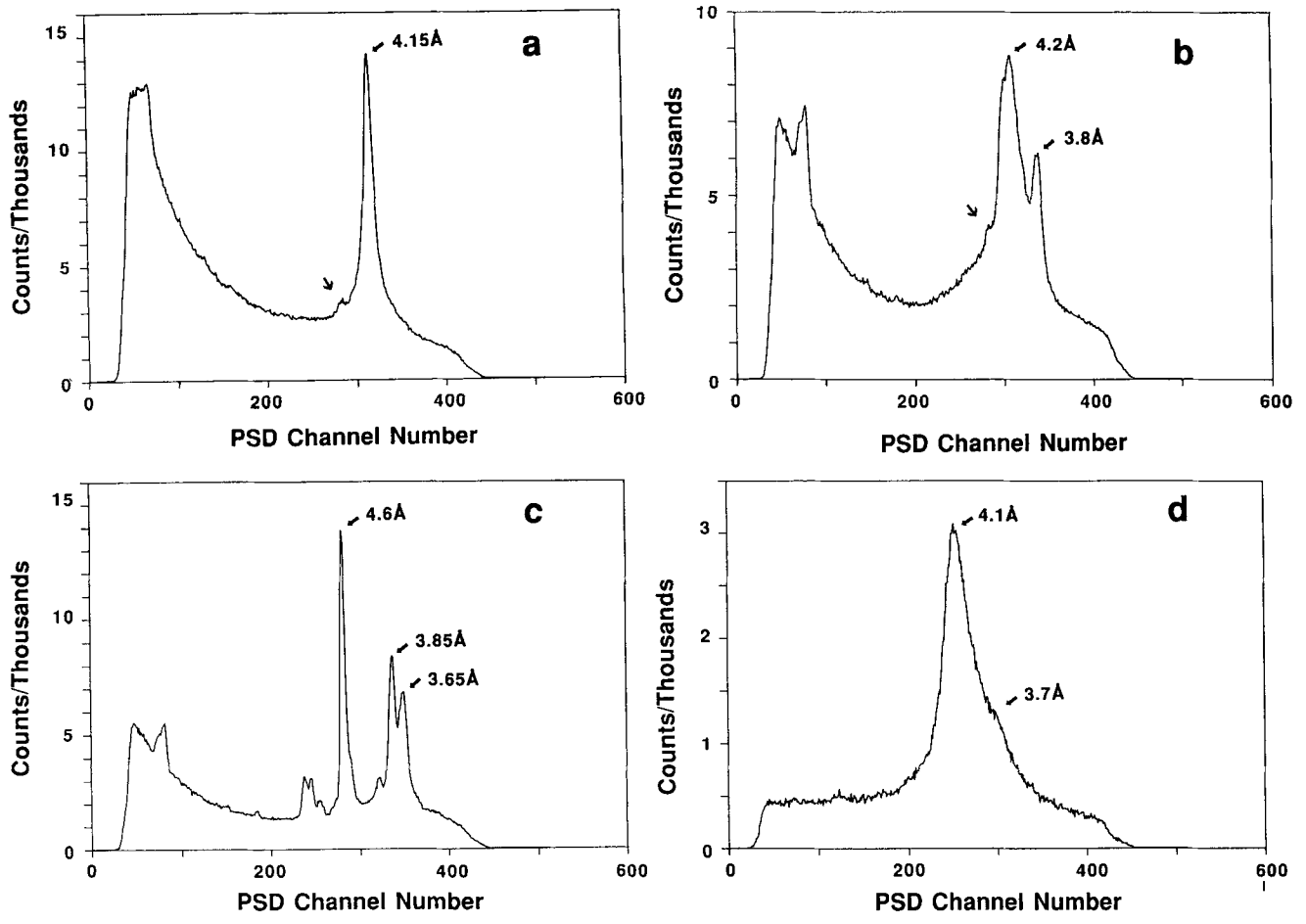

FIG. 1. Wide-angle X-ray diffraction patterns of four crystal forms of chain-deuterated tripalmitin. (a) α form. A single peak with a Bragg spacing of 4.15 Å. (b) β' form. Dominant peak and one subsidiary peak with Bragg spacings of 4.2 and 3.8 Å, respectively. (c) β form. Dominant peak and two subsidiary peaks with Bragg spacings of 4.6, 3.85 and 3.65 Å, respectively. (d) Sub-α form at −130°C. Dominant peak and a broad shoulder with Bragg spacings of 4.1 and 3.8 Å, respectively. Note that the position-sensitive detector is positioned differently here than in (a) through (c).

Different crystal forms can be detected simultaneously in the same pattern; in this case, the peak areas are a measure of the amount of each form present.

Fourier-transform infrared (FT-IR) methods. FT-IR spectra were obtained with a Mattson Cygnus 100 spectrometer interfaced to an IR-PLAN infrared microscope by means of an external beam port (Mattson Instruments, Inc., Madison, WI). The microscope interface was equipped with a mid-band mercury-cadmium-telluride detector permitting operation in the 600 to 4,000 cm^{-1} region. Infrared spectra were the result of Fourier transformation of 128 co-added interferograms at 1 cm^{-1} resolution with triangular apodization.

Polymorphs were prepared for FT-IR by following the same protocols as for NMR and X-ray diffraction. A small amount of material was melted on a piece of aluminum foil or a silver chloride disc (1 mm × 13 mm), the sample quenched in water at the appropriate temperature, then mounted in a variable-temperature microscope stage (MMR Technologies, Inc.) at 20°C. The variable-temperature stage is equipped with a heater and a Joule-Thomson refrigerator that allows the temperature of the stage to be controlled between 100 and −193°C *via* an MMR K-20 temperature controller, which is operated through a microcomputer. Both transmittance and reflectance modes were used to produce infrared spectra.

Deuterium solids NMR methods. ^2H NMR spectra were recorded at 61.4 MHz on a Bruker MSL400 NMR spectrometer. Sample temperature was regulated by a Bruker BVT-1000 temperature controller by reheating a stream of cold nitrogen gas. A cylindrical sample of 8-mm length and 5-mm diameter (approximately 100 microliters volume) was placed in the center of a 14-mm long solenoid coil oriented with the coil axis perpendicular to the field of the superconducting solenoid. Prior to data acquisition the amplitude and phase of the radiofrequency pulses of each of the four quadrature phases were adjusted according to the method of Gerstein (39). The transmitter offset and receiver phase were adjusted to minimize the signal detected in one of the two channels of the quadrature receiver.

^2H spectra were acquired by a quadrupole-echo pulse sequence with two 90° pulses: ($\pi/2$-τ_1-$\pi/2$-τ_2-acquire-relaxation delay) (40,41). Phase alternation of the echo pulse

was superimposed on quadrature phase cycling of both pulses. The typical 90° pulse length was 2 μs, the interpulse spacing was 17 μs, data acquisition was begun 15 μs after the end of the second pulse, and the relaxation delay between repetitions was usually 20 s. Inversion recovery T_1 measurements were made by adding a 180° pulse and a relaxation delay before the quadrupole echo sequence (41,42).

Echo transients were digitized at 0.2 μs dwell time and stored as 2K data sets. Typically 16 to 64 acquisitions were co-added for the chain-deuterated tripalmitin and 200 scans for the glycerol-labelled tripalmitin. Data were left shifted prior to Fourier transformation until the maximum on the quadrupolar echo was the first point in the data set, then a 400 or 500 Hz exponential line broadening was applied, and the data were zero-filled to 8192 points. Small zero-order phase corrections to the spectrum were sometimes required. No artificial symmetrization of the spectrum was performed.

^2H NMR theory and lineshape simulations. The deuterium NMR spectrum is dominated by the interaction between the nuclear electric quadrupole moment of this spin 1 nucleus and the electric field gradient sensed at the nucleus (28,43). Though the chemical shift contribution exists, it is essentially the same as that for protons on a ppm scale. At the field strength used here, the deuterium shift range is less than 600 Hz and is therefore small compared to the quadrupole contribution to the line widths in the solid. The electric field gradient tensor is usually well approximated by axial symmetry in a carbon-deuterium bond. Thus, each orientation of a bond in a molecule should produce two resonances at two discrete frequencies, corresponding to the two allowed transitions for a spin-1 nucleus. However, for a polycrystalline sample, all orientations of this gradient are represented. The resulting spectrum is a superposition of contributions of all orientations. Because the deuterium NMR spectrum arises from two transitions, the polycrystalline spectrum is the sum of two patterns related to one another by symmetry. The polycrystalline spectrum, or powder pattern, can be very wide (270 kHz). However, motions that mix orientations on a time scale short compared to the reciprocal of the line separations cause significant powder pattern line-shape changes. Fast motions about a single axis, such as rapid rotation of methyl groups, preserve the axial nature of the powder pattern, but reduce its width. Fast motions of other types may cause changes in both line-shape and width. Detailed line-shape analysis generally requires comparison of experimental line shapes with those computed from various motional models.

RESULTS AND DISCUSSION

In this section we begin by presenting evidence that the deuterated tripalmitin samples can be prepared in crystal forms that are the same as unlabelled tripalmitin, as judged by X-ray diffraction and infrared spectroscopy. The deuterium NMR spectra of tripalmitin in the solid state are then presented with analysis of line shapes in terms of simple models for molecular motion, Finally, the detailed structural and dynamical behavior of the α and β forms at low temperatures and the spontaneous transition of α to β at higher temperature are described.

Verification of crystal forms. Representative X-ray diffraction patterns recorded from an NMR sample at 20°C are shown in Figure 1. The α form gives a single, moderately broad peak at 4.15 Å (Fig. 1a). A small peak at 4.6 Å shows that a few percent β crystals have formed at the same time (arrow). The β′ form (Fig. 1b) gives one peak at 4.2 Å, *i.e.* slightly to the left of the peak in (a), and a second peak at 3.8 Å. Finally, the β form gives a strong peak at 4.6 Å and two more at 3.85 and 3.65 Å (Fig. 1c); the absence of peaks in between shows that neither α nor β′ crystals are present in this case.

Figure 2 shows infrared spectra of α, β′ and β chain-deuterated tripalmitin and unlabelled tripalmitin. It is evident from Figure 2d, which is an expansion of the 720-cm^{-1} region, that α crystals were produced when chain-deuterated tripalmitin was heated to 95°C, quenched at 30°C and then observed at 20°C. The single band near 720 cm^{-1}, attributed to the main rocking-twisting CH_2 mode, and the absence, even at −193°C of numerous bands present in the β and β′ polymorphs (compare Fig. 2a to Fig. 2b and c) is characteristic of the α form in unlabelled tripalmitin (44,45). The β′ form of chain-deuterated tripalmitin was studied by heating the sample to 95°C, quenching at 46°C for five minutes and observing at 20°C or −193°C (Fig. 2b). For unlabelled tripalmitin at −193°C, Figure 2f, the closely spaced bands at about 720 cm^{-1} and 730 cm^{-1} and bands in the 800 to 1000-cm^{-1} region (not shown) uniquely indicate β′ crystals (20,46–48). A single band at 720 cm^{-1} together with a pair of strong bands at about 900 cm^{-1}, demonstrates the presence of β crystals (Fig. 2c). These were produced when β′ crystals were heated to 62°C for one hour.

Quadrupole echo deuterium NMR spectra of α, β′ and β forms of chain-deuterated tripalmitin. Quadrupole echo deuterium NMR spectra of the three polymorphic forms of the chain-deuterated tripalmitin at 20°C are shown in Figure 3. These spectra clearly demonstrate that, at a temperature below the lowest melting temperature of the three polymorphs and low enough to inhibit any solid-solid transition, the degree of motional averaging of the ^2H NMR spectrum depends on the polymorphic form of the crystal (35). The spectrum of the β polymorph indicates a minimal degree of motional averaging. This spectrum is the sum of two powder patterns: a wider, more intense methylene deuteron pattern with a horn-to-horn splitting of 118.4 kHz, and a narrower, less intense, methyl powder pattern with a horn-to-horn splitting of 34.8 kHz. The methylene powder pattern is only about 7 kHz or 6% narrower than the rigid limit value of about 125 kHz (28), which is consistent with highly restricted molecular motions. Free rotation of the CD_3 group about the C_ω-$C_{\omega-1}$ bond would yield a threefold narrowing from the rigid limit. One-third the width of the rigid limit is 42 kHz or about 7 kHz more than the observed methyl value. That the CD_3 powder pattern width is narrower than 42 kHz indicates that there is more motion present than rotation about the methyl C_3 axis at the end of the alkyl chain.

By comparison, the ^2H spectra of the α and β′ polymorphs are narrower and have a different shape. These spectra also result from the superposition of methyl and methylene contributions. The spectrum for the α form indicates more motional averaging, at least for the methylene deuterons, than is seen for the β′ form. We could not reproduce the β′ spectrum by a linear combination of the β and α spectra, confirming that the third crystal form

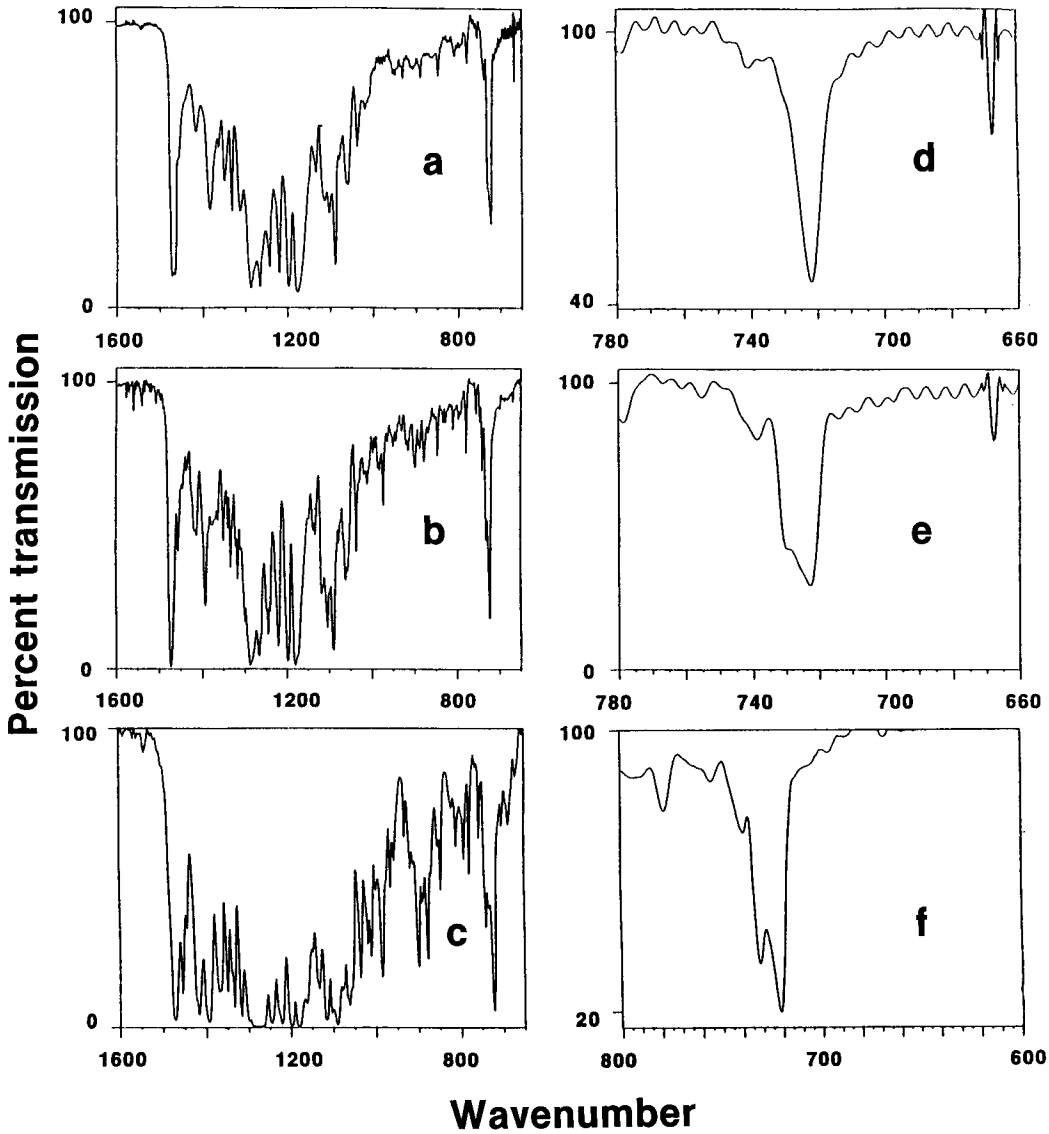

FIG. 2. Fourier-transform infrared spectra of unlabelled tripalmitin and chain-deuterated tripalmitin. (a) Labelled α at −193°C. (b) Labelled β' at −193°C. (c) Labelled β at −193°C. (d) 720-cm^{-1} region of labelled α at 20°C. (e) 720-cm^{-1} region of labelled α at −193°C. (f) 720-cm^{-1} region of unlabelled α tripalmitin at −193°C.

indeed was formed. The spectra of the α and β' polymorphs indicate considerable motional averaging in comparison with β.

Relation of motion to geometric and intermolecular constraints in the crystallographic lattice. The conformation of the triglyceride molecule has been determined in the β (triclinic) form by X-ray structure analysis (49). In particular, the all-*trans* methylene chains were found to be in close and regular contact. In contrast to the β form, the crystal structure of the α (hexagonal) form has not been solved. We note that the hexagonal symmetry of the α form relates to packing of the individual acyl chains, *i.e.*, it does not reflect the existence of the glycerol moiety at all. The hexagonal packing requires a chain cross-section of either circular, triangular or hexagonal symmetry. None of these fits the precise shape of an all-*trans* methylene chain. The hexagonal packing, taken together with the paucity of X-ray reflections from the α form, in fact suggests irregular contacts between chains such that a cylindrical shape applies, on average. On this basis one might have anticipated less regular, larger-amplitude structural fluctuations in α than in β chains. Both the NMR observations on relaxation rates at 20°C (Fig. 4) and the relative thermodynamic stabilities of these forms confirm this picture. Taken together, the volumetric, X-ray and NMR observations indicate irregular and rapidly fluctuating conformations for the acyl chains in the α form. While chain motions also occur in the β form (49), evidently these are more constrained than in the α form (Fig. 3).

Although the complete crystal structure of the β' form.

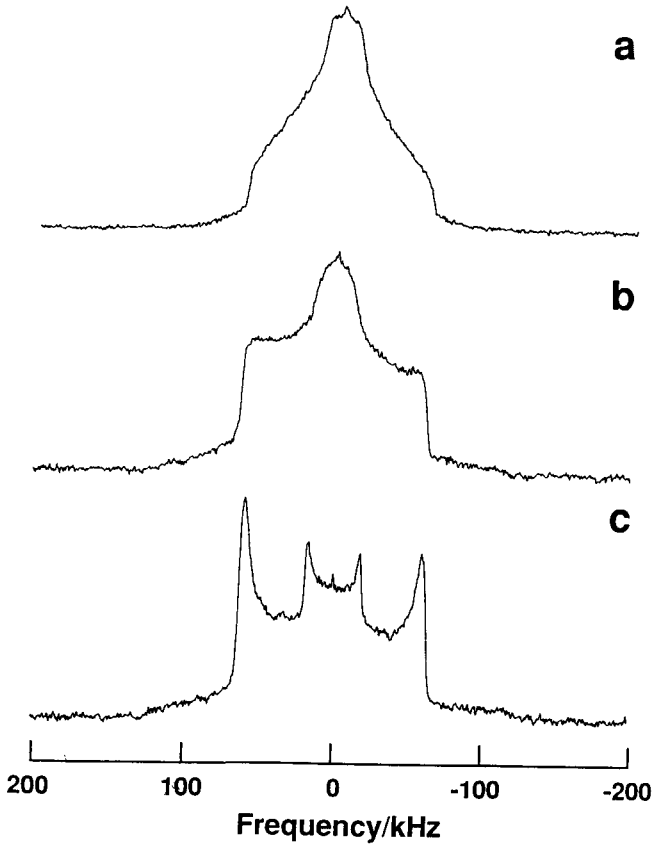

FIG. 3. Quadrupole echo ^2H nuclear magnetic resonance spectra of chain-deuterated tripalmitin at 20°C, prepared in three different crystalline forms according to methods in the text: (a) α (hexagonal) form; (b) β' (orthorhombic) form; (c) β (triclinic) form.

has not been solved, X-ray observations have been used to categorize acyl chain packing in the β' form, which is defined by X-ray short-spacing reflections at about 3.8 Å and 4.2 Å. These are the values encountered in long-chain compounds known to pack in an orthorhombic subcell. In fact, from the limited X-ray data available, the acyl subcell appears to be very nearly orthorhombic, as in triundecanoin (50), LML ($C_{12}C_{14}C_{12}$) (51) and tripalmitin (52). The β' subcell is commonly regarded as being regularly and closely packed, based on comparisons among many lipids (ref. 6, Chapter 2). Based on this, motions would be expected to be similarly restricted in the β' and β forms, and less restricted in the α form. The NMR data at 20°C (Fig. 3) suggest instead that motions in β' and α are similar. The NMR data at lower temperatures also show that motion in the α form can become about as restricted as in the β form (compare Fig. 9a to Fig. 3c). An explanation was sought for the 20°C data.

It is well known that a crystal lattice may expand as the temperature increases with no change in symmetry (4). In fact, the volume per CH_2 group for triglycerides in various polymorphic forms increases gradually as temperature is increased, up to the melting temperature, at which point there is a discontinuous jump to the value for the liquid (ref. 6, p. 31 and Table 2–6). For tripalmitin, volumetric data are only available for the liquid and β forms. However, dilation curves (specific volume *vs.* temperature) have been published for the three polymorphs of tristearin, a near homolog of tripalmitin (ref. 6, p. 370). The specific volume of α is only slightly greater than that of β' tristearin (both are close to 1 mL/g). This relationship holds over the range from 10°C to their melting points, both of which are above 50°C. However, the specific volumes increase gradually with temperature. These specific volumes both are substantially greater (about 3%) than that of β tristearin, over the same temperature range. Assuming similar volumetric behavior for tripalmitin and assuming that mobility is dominated by available volume, we would predict that the NMR line shapes of α and β' will be similar to one another, since the average volumes available to their chains are similar. Further, we would predict that the NMR line shapes of α and β' will both show substantially more evidence of motional averaging than β, because the specific volumes of α and β' are significantly larger than that of β. The results of Figure 3 are consistent with this explanation.

In terms of all three measures—crystallography, thermodynamics and molecular dynamics—the β' form is intermediate between the α and β forms. The observation that the dynamics of the β' form are more like α than β (Fig. 3) illustrates that NMR observations offer unique insights and that detailed volumetric data from X-ray and density measurements are valuable for interpretation of measurements of molecular mobility.

Spin-lattice relaxation. As we have discussed, changes in ^2H line-shape with crystal form are produced by motions in the tens to hundreds of kHz range, of the same order of magnitude as the width of the powder pattern, or faster. High-frequency motions may be probed by measuring the deuteron spin-lattice relaxation time from an inversion-recovery quadrupole echo sequence. The deuteron T_1 is sensitive to fluctuations in the electric field gradient near the Larmor frequency, in this case 61.4 MHz.

Results of quadrupole-echo inversion-recovery measurements of deuterium T_1 for the α and β polymorphs are shown in Figure 4. Note that inversion of the wings of the methylene powder pattern of the β polymorph is incomplete (Fig. 4, lowest curve), even with the 4-μs π-pulse employed. For the β form, the methylene spin-lattice relaxation is relatively slow, corresponding to a T_1 of 18.4 s for nuclei for which the C-D bond vector is perpendicular to the magnetic field, *i.e.*, the sharp horns. T_1 for the methyl deuterons, approximately 0.25 s in the β form, is significantly shorter because of the methyl rotation. For the α form, it is not possible to deconvolute the methyl and methylene T_1's; however, inspection of the partially relaxed spectra suggests that they must be similar. A composite methylene and methyl T_1 may be calculated at the center of the powder pattern; using this method, T_1 is 0.16 s for the α form (Fig. 4a), and of the order of 0.2 s for the β' form (data not shown). Clearly, the lattice geometry of α and β' forms at 20°C permits methylene motions near the Larmor frequency that produce efficient longitudinal relaxation. In the β form, ^2H spin-lattice relaxation is about 100 times less efficient, which indicates a considerable reduction of motion near the Larmor frequency.

In a study by Norton *et al.* (23), ^1H spin-lattice relaxation measured at 60 MHz was more than ten times as

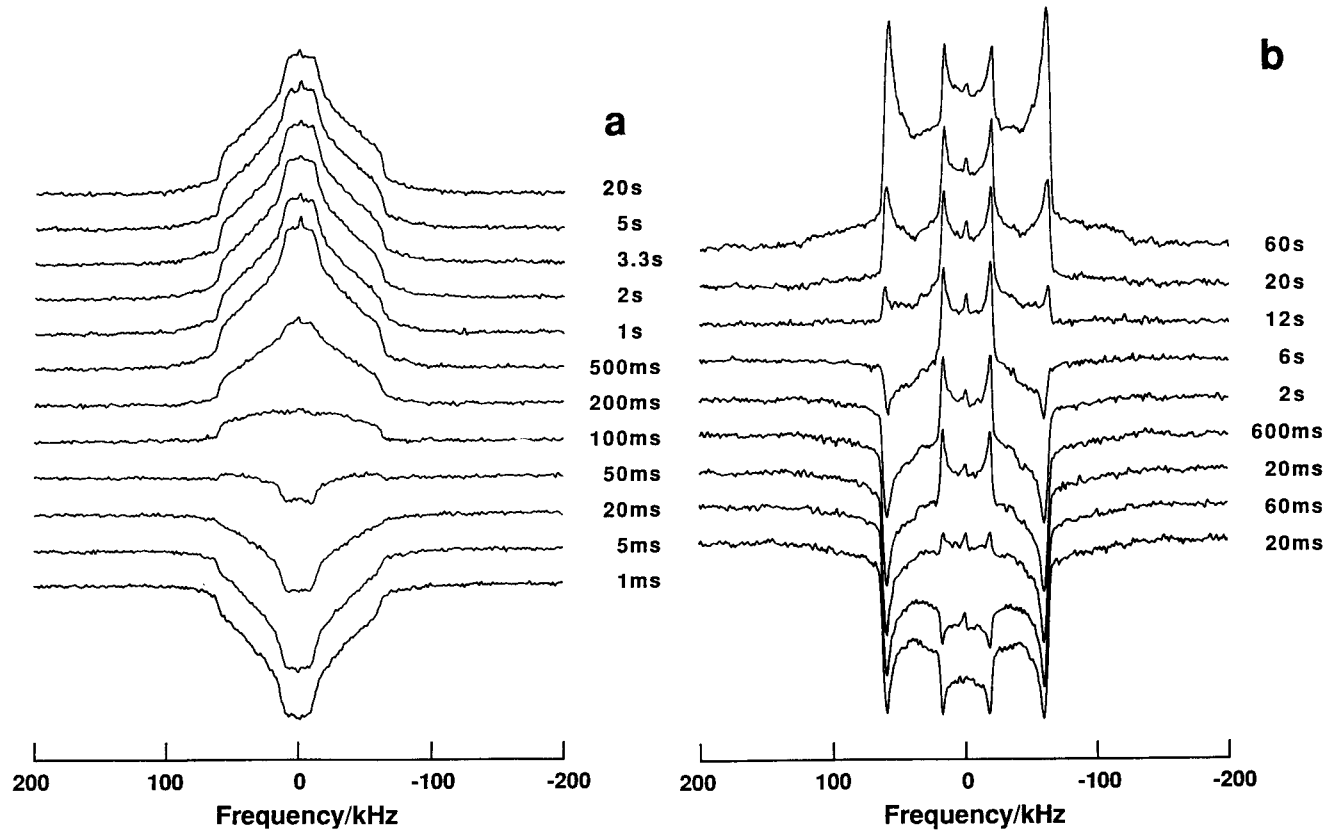

FIG. 4. Inversion-recovery quadrupole echo ^2H nuclear magnetic resonance spectra for measurement of relaxation time T_1 (^2H) of chain-deuterated tripalmitin at 20°C. For each spectrum the delay time between the 180° pulse and the quadrupole echo measuring sequence is noted: (a) α (hexagonal) form; (b) β (triclinic) form.

efficient for the α form as for β. However, those authors pointed out that the shorter T_1 for α could arise from a single molecular site, *i.e.*, the methyl group, because due to efficient spin diffusion in the strongly coupled ^1H system, the most mobile site may dominate overall ^1H relaxation. The possibility that the shorter T_1 for α is due to a difference in methyl motion between the two polymorphs is eliminated by the deuterium results. That is, for the methyl group, rotation about the C-C bond axis is always present, yielding efficient relaxation behavior in all three crystal forms, whereas the methylene groups have relaxation that truly depends on polymorphic form.

Interpretation of the line shape of the α polymorph. Interpretation of the α line shape is complicated by the fact that the spectrum is a sum over the line shape from deuterons at positions all along the fatty acid chain. We note that X-ray diffraction analysis of the β form found increasingly large thermal motions as the methyl group terminating each chain is approached (49). This result suggests that dynamics vary as a function of chain position. An obvious explanation for the X-ray observations is that the methyl group interacts with neighboring chains *via* relatively weak van der Waals forces, whereas the carbonyl end of the same chain is covalently bonded to the glycerol backbone and thereby restricted. The α and β' forms should behave similarly. Thus, for triglycerides, the first step toward a more detailed motional picture would be to obtain line shape and relaxation data from triglycerides labelled at specific sites along the hydrocarbon chain, a strategy that has worked well in membrane studies (27–29).

Nevertheless, it is useful to consider in a general fashion what rates and geometries of motion could give rise to the observed α line shape. First, note that the T_1 relaxation time for the α form suggests sufficient motion at the Larmor frequency to produce relaxation which is rapid compared to the β form. Second, we have examined the α line shape as a function of the spacing τ_1 between the two radio frequency pulses in the quadrupole echo sequence. No changes in the line shape (T_2 distortions) were observed for values of τ_1 between 17 and 102 μs (Fig. 5). This suggests that the motions responsible for the line shape are rapid compared to the time scale of the experiment, about 10^{-5} s (53). Thus, the relaxation data indicate that the motions responsible for the observed line shape are relatively rapid.

The line shape of the α polymorph at room temperature is similar to the fully anisotropic ($\eta^* = 1$, $\eta_Q^* = \nu_Q/2$) line shape that results from rapid exchange between two sites for which the orientation of the C-D bond axis differs by the tetrahedral angle. An attempt was made to simulate the observed powder pattern for the α form on the basis of a simple two-site tetrahedral jump, explicitly taking into account the finite length of the pulses and the echo time

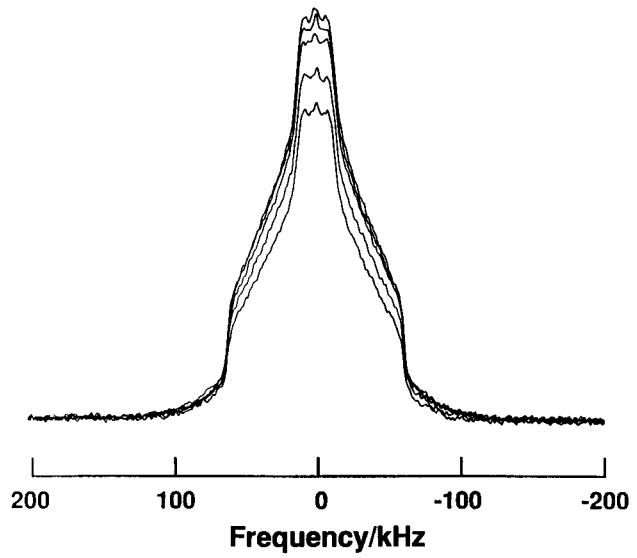

FIG. 5. Quadrupole echo ^2H nuclear magnetic resonance spectra of chain-deuterated tripalmitin, prepared in the α form, at 20°C, as a function of the interval τ_1 between pulses. Spectra with τ_1 values of 17 μs (largest intensity), 27 μs, 42 μs, 72 μs and 102 μs (smallest intensity) are shown.

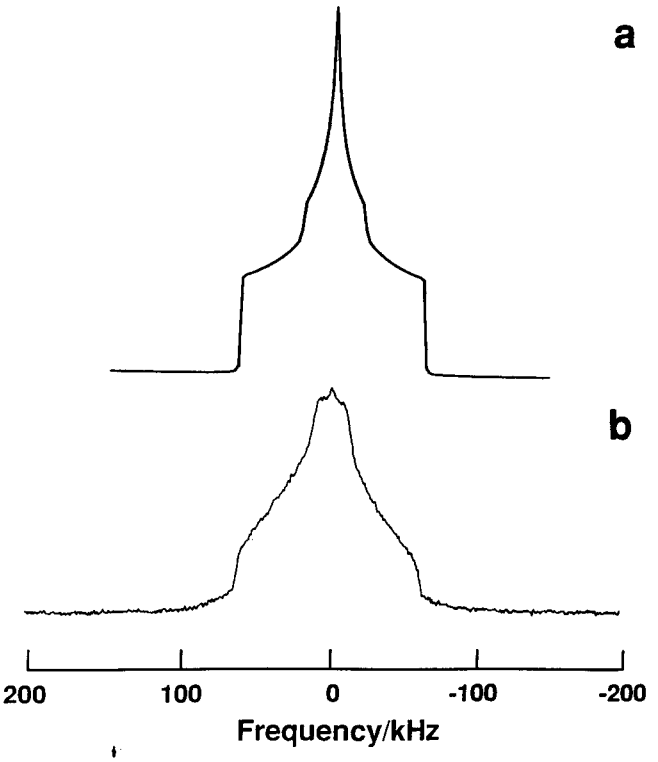

FIG. 6. (a) Simulation of the quadrupole echo spectrum (τ = 17 μs) of the α form of chain-deuterated tripalmitin, assuming each C-D bond undergoes exchange between two equally populated orientations 109.5° apart, at a rate of 10,000 s^{-1} for the methylene deuterons and 10,000 s^{-1} for the methyl deuterons, and that rapid rotation of the methyl group further reduces the width of the methyl powder pattern by a factor of three. (b) Quadrupole echo ^2H nuclear magnetic resonance spectrum (τ_1 = 17 μs) at 20°C of chain-deuterated tripalmitin prepared in the α polymorph.

employed (Kennedy, S.D., unpublished dissertation). The two-site tetrahedral jump model has been extensively applied to analysis of ^2H line shapes of alkane systems (*e.g.*, 54,55). Methylene and methyl line shapes were simulated separately, and the final spectrum was computed as a weighted sum of the individual simulations. A uniform jump rate at all methylene positions along the hydrocarbon chain was assumed. For the methyl simulations, it was also assumed that rapid reorientation about the terminal C-C bond reduces the quadrupolar interaction by a factor of 1/3.

Results that approximate the major features of the α spectrum (width and appearance of wings) are obtained for jump rates on the order of 1×10^4. Figure 6 compares the experimental spectrum to a spectrum simulated with a jump rate of 1×10^4 for the methylene deuterons and 2×10^4 for the methyl deuterons. However, no combination of methylene and methyl jump rates reproduced the observed pattern in detail. The major difficulties are that the central portion of the pattern is too intense in the simulations, and there is residual intensity in the observed powder pattern on both sides of the steep edges that is not consistent with the rapid tetrahedral jump model. Faster motions, as suggested by the relaxation data, yield line shapes that converge to the fully anisotropic powder pattern, exacerbating differences between the observed and calculated spectra. These differences argue against a tetrahedral jump model and imply that dynamical heterogeneity may be an important factor in these systems. Here dynamical heterogeneity may imply differences in motions at different positions along the chain or heterogeneity of motion at a single chain position.

The two-site jump model has also been applied in more general forms, permitting unequal population of the two sites (56,57) and deviations from the tetrahedral angle (57). Similar line-shape changes may be generated by modeling the NMR data based on a distribution of angles (58). Such line shapes have been modelled by using continuous reorientation of the C-D bond about a director axis in a potential well (58–60). For methylene deuterons in crystalline nylon 66, Hirschinger *et al.* (53) used rapid librations described by a Gaussian distribution of azimuthal angles of standard deviation $\Delta\theta$. To fit the observed line shapes and relaxation behavior, it was necessary to assume a spatially inhomogeneous distribution of $\Delta\theta$. Thus, the observed line shapes do not uniquely identify the type of motion present. Although the two-site jump model is apparently simple when viewed from the point of view of an isolated C-D bond, executing a tetrahedral jump for an alkane chain constrained in a crystal lattice would require the concerted motion of many atoms. Rapid, continuous small-angle reorientations might be a more physically reasonable motional model for alkyl chains constrained by a crystal lattice.

In summary, the relaxation behavior of the α spectrum indicates that the motions responsible for the line shape are fast on the time scale of the experiment. However, a wide variety of motional models may be used to fit such a line shape. To obtain more detailed information about

the motion, it would first be necessary to prepare triglycerides that are specifically labelled with deuterium. The line shape, τ_1 dependence of the line shape, and of T_1 as a function of temperature, could then be used as a basis or more detailed interpretation of the motions involved.

Interpretation of the line shape of the β′ polymorph. Qualitatively similar conclusions apply to interpretation of the line shape of the β' polymorph. We have not measured this powder pattern as a function of τ_1, but T_1 is also much shorter than the T_1 for the β polymorph. Thus, the motion responsible for averaging the powder pattern is probably also rapid compared to the time scale of the experiment. However, the motion is less effective in averaging the powder pattern than the motion in the α form. The singularities in the powder pattern remain more prominent, and there is more intensity left in the wings of the pattern. The simplest explanation is that the motion in the β' polymorph is of smaller amplitude than the motion in the α polymorph.

Motions in the glycerol backbone. Room temperature spectra of the β and α forms of the glyceryl-deuterated tripalmitin are shown in Figure 7. Superficially, the spectra appear to be composed of a single powder pattern, although each represents the sum of the signals from the five labeled deuterons. Indications of shoulders on the outer edges of the horns could originate from differences in the powder pattern of individual deuterons, slight deviations from the assumption of a negligible asymmetry parameter for the field gradient tensor, or heterogeneity in the motional behavior of triglyceride molecules. Apparently, however, the motions of the five deuterions in the glycerol backbone are similar within each polymorph.

For the β spectrum the horn-to-horn separation is 116.6 kHz, again slightly reduced from the rigid limit, which suggests minimal motional averaging. For the α form, reduced intensity of the horns suggests additional dynamical averaging, but the motional difference between the α and β forms is much less pronounced for the backbone than it is for the chains.

Physically reasonable models for the motions that cause slight motional averaging in the backbone resonances must take into account at least two factors: (i) Each backbone carbon is attached to several bulky constituents; (ii) the backbone is known to play an important role in defining and stabilizing the crystal lattice (ref. 6, Chapter 5). Thus, the most reasonable models to account for observed ^2H NMR line shapes would necessarily involve the concerted motions of many atoms in the vicinity of the C-D bond of interest.

For the α form, comparison of the spectrum of backbone atoms (Fig. 7) with the spectrum of methylene chain atoms (outer shoulders in Fig. 3) indicates that the major motions are confined to the hydrocarbon chains. For the β form, deuterium spectra show minimal motional averaging for either glyceryl or acyl chain atoms; however, no conclusion may be drawn about possible coupling between glyceryl and acyl chain motions.

Isothermal solid-solid transition from α to β. Solid-solid transitions between polymorphic forms of triglycerides are well known and may be observed as characteristic changes in the X-ray pattern, infrared spectrum, density and calorimetric behavior. Because the kinetics of these solid-solid transitions are strongly temperature-dependent

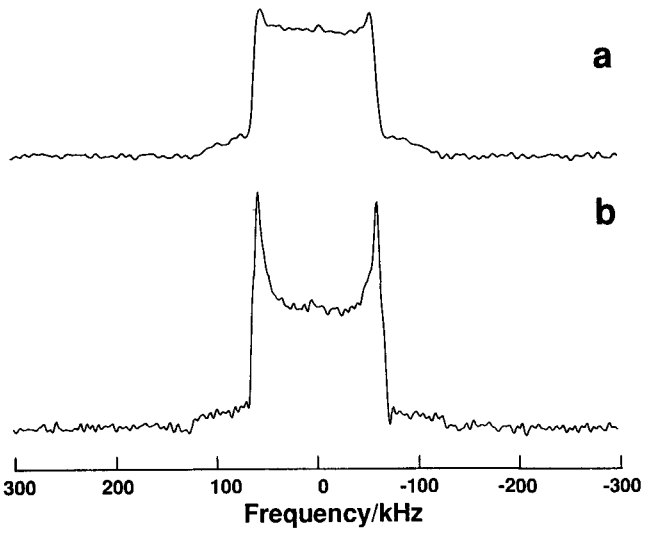

FIG. 7. Quadrupole echo ^2H nuclear magnetic resonance spectra at 20°C of glyceryl-deuterated tripalmitin, prepared in two different crystalline forms: (a) α (hexagonal) form; (b) β (triclinic) form.

(62-64), the time scale can be altered. Concomitant changes in the motional state of the triacylglycerols may then be conveniently monitored during the transition by ^2H NMR spectroscopy.

Figure 8 shows the ^2H NMR spectrum of chain-deuterated tripalmitin at half-hour intervals during the course of the α to β solid-solid transition at 35°C. The change in acyl chain mobility during the transition is reflected in the spectra. Comparison of horn regions of both methyl and methylene deuterons of the 12.5-h spectrum with the spectrum of the pure β form at 20°C (Fig. 3) suggests that the transition is not quite complete after 12.5 h at 35°C. This observation correlates with (i) an effect in the X-ray pattern, where the peaks in the β pattern show significant broadening, depending on sample preparation and aging, and (ii) a melting enthalpy that is below the published value (6). The potential for measuring the extent and kinetics of solid-phase transitions from ^2H line-shape changes is clear.

Reversible thermal transition of α to sub-α upon cooling. In principle, freezing acyl chain motions by lowering the temperature should increase the rigid limit character of any spectrum. Lowering the temperature of a sample in the α form, however, produces a material with crystallographic and vibrational characteristics that distinguish it from the α, β' and β forms. This material has been designated "sub-α" (8,64,65). These characteristics were measured for the deuterated tripalmitin sample as follows.

X-ray diffraction observations. A sample of chain-deuterated tripalmitin was prepared in the α form in a thin-wall X-ray capillary following the protocol in Experimental Procedures, and then this sample was exposed for X-ray diffraction at low temperatures. As shown in Figure 1d, when the α form of chain-deuterated tripalmitin is cooled to −120°C, a shoulder appears to the right of the original α peak, and the peak itself is broadened asymmetrically compared to the room-temperature pattern from the same specimen. The shoulder shifted gradually

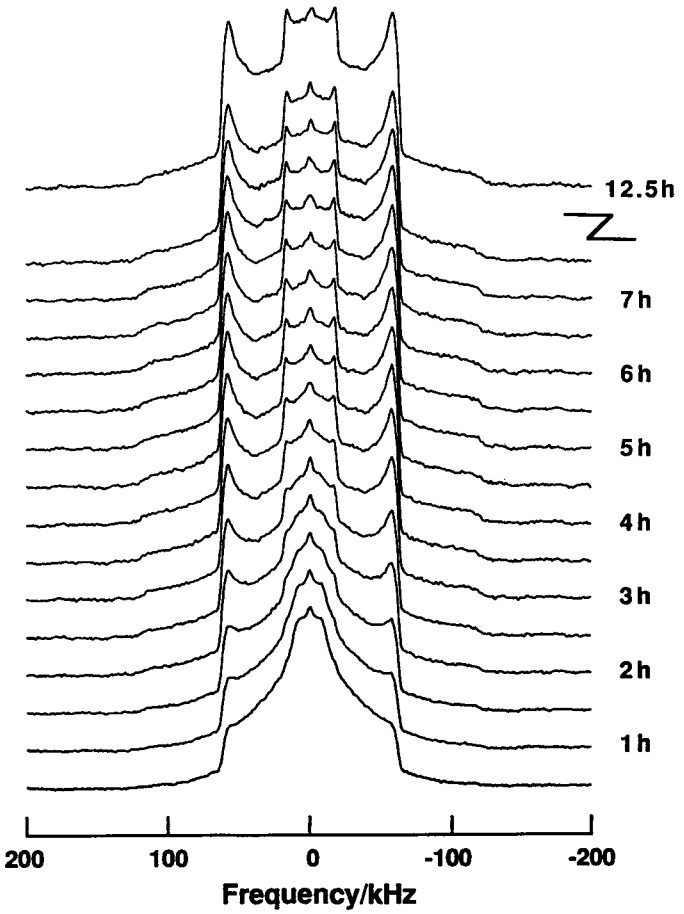

FIG. 8. Solid-solid transition from α to β in chain-deuterated tripalmitin at 35°C. The quadrupole echo ^2H nuclear magnetic resonance (NMR) spectrum of a sample prepared in the α form and held at 35°C in the NMR probe was recorded at half-hour intervals over a 12.5-h period. Spectra obtained at half-hour intervals are shown.

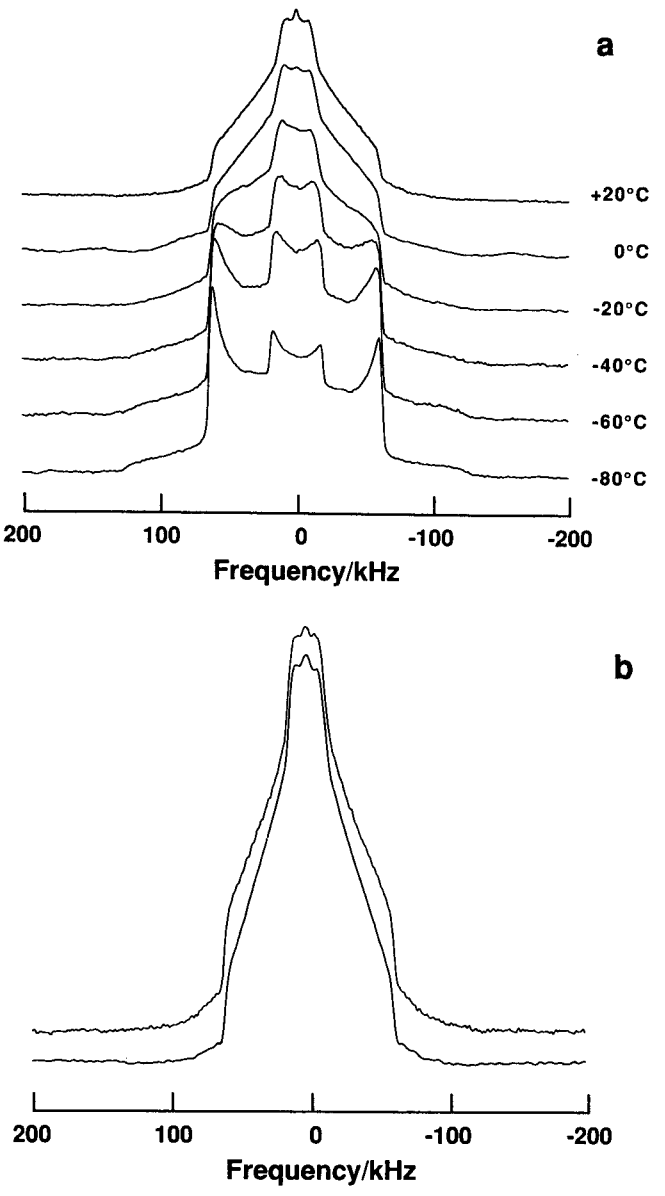

FIG. 9. Reversible conversion of α to sub-α form obtained upon cooling chain-deuterated tripalmitin. (a) A sample prepared in the α form was cooled in the nuclear magnetic resonance (NMR) probe, and quadrupole echo ^2H NMR spectra were acquired at successively lower temperatures, as indicated. (b) At the end of the experiment the sample was again warmed to 20°C. The final spectrum obtained (top) was identical to the initial 20°C spectrum (bottom).

(patterns not shown) when the temperature was lowered in steps as in the NMR and IR experiments, becoming clearly defined at about −60°C and more pronounced as the temperature approached −100°C. At −120°C, the dominant peak has a Bragg spacing of about 4.1 Å, and the shoulder has a Bragg spacing of about 3.8 Å (Fig. 1d). The latter value is similar to the Bragg spacing of the second peak from β' chain-deuterated tripalmitin at 20°C however, at no temperature studied did the shoulder become a well-defined peak, unlike the case for the β' crystals in Figure 1b. When the specimen was warmed to 20°C, the shoulder went away and a single, symmetric peak at 4.15 Å was seen as in Figure 1a, demonstrating the reappearance of the α crystal lattice. Thus the α to sub-α transition was rapidly and fully reversible.

Infrared observations. The main rocking mode is shifted from 720 to 525 cm^{-1} when methylene chains $[(-CH_2-)_n]$ are replaced by deuterated methylene chains $[-CD_2-)_n]$ (44). The presumptive 525 cm^{-1} band from the chain-deuterated tripalmitin used in the present study was not detectable because of the limited range of the mid-band MCT detector as well as the zinc selenide windows in the variable temperature microscope stage. When the α form of chain-deuterated tripalmitin was cooled from +20 to −193°C, the 720 cm^{-1} band gradually split, as observed previously (66,67); the splitting seen in Figure 2e characterizes the sub-α form. A similar observation is made for nondeuterated tripalmitin (Fig. 2f). The split band suggests an orthorhombic structure similar to β' (Fig. 2b) (5). Nonetheless, the sub-α form clearly is not β', first because bands in the 800- to 1000-cm^{-1} range, characteristic of β' triglycerides (Fig. 2b), are absent (Fig. 2a); and second, because the α spectrum is recovered upon warming to +20°C (Fig. 2d). This recovery would not occur if a transition to the thermodynamically more stable β' form had been achieved.

NMR observations. Figure 9 illustrates the changes in

the ^2H NMR spectrum which accompany the cooling of the α form from room temperature to −80°C. As the sample is cooled, there is a gradual transition from the motionally averaged pattern to one indicating nearly rigid chains. The transition is reversible, *i.e.*, the spectrum obtained upon warming of the sample to 20°C was indistinguishable from the original. Thus, the change in chain dynamics accompanying the formation of the sub-α form is readily observed by ^2H NMR.

Although the spectrum observed at −80°C is similar to that observed for the β form near room temperature, the ^2H NMR spectra indicate only that motion decreases as temperature is lowered. There is no indication of an α to β transition, which would be irreversible.

Combined X-ray, infrared and NMR results. The changes in X-ray pattern and infrared spectrum are consistent with a shift of some fraction of acyl chains from hexagonal packing toward orthorhombic packing (4). Based on the NMR observations of differences between α and β' forms at 20°C, this structural shift should be accompanied by a shift toward more restricted molecular motion. The NMR spectra obtained while cooling the α form to −80°C, however, indicate a much greater restriction of motion than that expected solely on the basis of lattice geometries at 20°C.

We speculate that the additional restriction may be caused in part by a decrease in volume. While the coefficients of thermal expansion for α and β' tripalmitin are not tabulated, those for tristearin are: α, 3.2×10^{-4} mL/g°C (over the range −38 to −33°C); β', 2.9 (−38 to −33°C); and β, 2.3 (−38 to −20°C) (ref. 6, pp. 368–369, Table 10-3). A volume decrease of about 2 to 3% can be roughly estimated for cooling α tristearin from +20 to about −38°C. This is comparable to the difference in volume between the α and β forms at temperatures in the 10 to 50°C range (ref. 6, p. 370, Fig. 10–16). Assuming tripalmitin volume behavior is similar to that of tristearin, acyl chains of tripalmitin may have less room to move during cooling. Measurements of volume are required to test this idea further.

Finally, lower temperature would also reduce the average kinetic energy of molecules with a concomitant reduction in amplitude and rates of motions.

What prevents the acyl chains from completing the transition to β'? Comparison with *n*-alkanes (4), which undergo a reversible transition from β' to α as temperature is increased, indicates that it is the glycerol backbone that prevents the chains from completing this transition as the temperature is lowered.

Effect of cooling the β (triclinic) form. The temperature dependence of the ^2H NMR spectrum of the chain-labelled tripalmitin in the β form is illustrated in Figure 10. Over a temperature span of 100°C, the width of both components in the powder pattern is observed to change only slightly. In terms of the rigid limit value of about 125 kHz, the outer pattern broadens from 94.5% of the rigid limit value to 98.4%, while the inner pattern broadens from 83.4% to 89.1%. As the temperature decreases and motions are reduced, the various methylene groups along the length of the hydrocarbon chain may become more motionally similar. As a result, the width of the outer horn, which is a composite of the horn of the individual methylene signals, is reduced, and the horn becomes higher relative to the intensity at the center of the pattern. This indicates that methylene motions of a rate and amplitude sufficient to average the powder pattern are more nearly frozen out at the lowest temperature of −80°C. At this temperature, methyl group motion continues to produce significant narrowing. The behavior of the β phase on cooling stands in marked contrast to the behavior of the α phase, in which a dramatic change in shape of the powder pattern accompanied the lattice distortion (Fig. 9). The β phase has a small coefficient of thermal expansion, 2.2×10^{-4} mL/g°C over the temperature range −38 to −18°C (ref. 6, pp. 368–369, Table 10-3); thus, cooling merely reduces the already limited motions in the dense lattice.

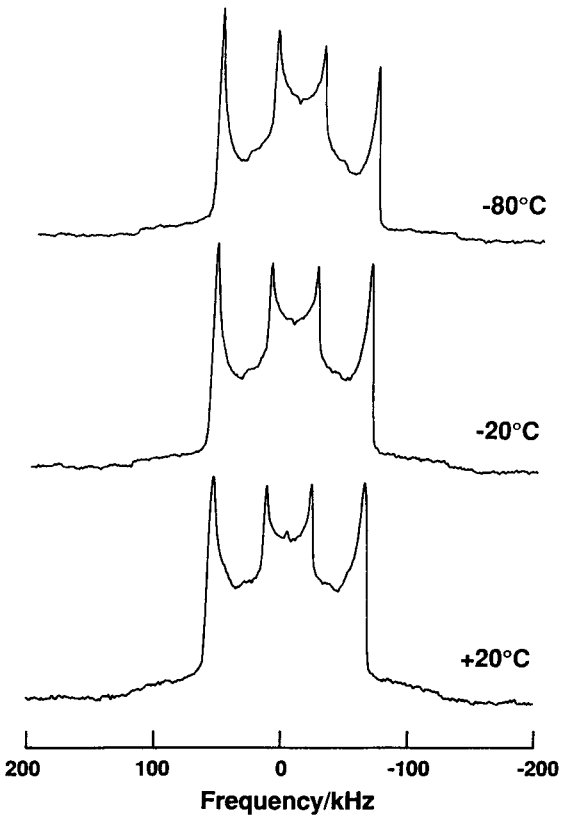

FIG. 10. Temperature dependence of the quadrupole echo ^2H NMR spectrum of chain-deuterated tripalmitin prepared in the β form.

In conclusion, deuterium solid-state NMR is shown to be useful for measuring the restricted motions of acyl chains and backbone glycerol in the polymorphs of a solid triglyceride. From rudimentary NMR theory, mobility is specified as highly restricted (small amplitude) rotations of C-D bonds at rates in the range of tens to hundreds of kilohertz, being much greater in α and β' than in β. In addition, restricted amplitude rotations with high frequency rates, in the range of tens of megahertz, are also much greater in α and β' than in β. The different spectra associated with the different crystal forms, as well as the changes in NMR line shape associated with thermally induced transitions, are consistent with the interpretation that larger volume (lower density) and a reduction in specific inter-chain contacts will dominate NMR-detectable mobility. Changes in mobility accompanying both the irreversible, thermally induced solid-state transition from

α to β, as well as the reversible transition to sub-α, may be monitored with this method. Extensions of these experiments might be used to establish parameters of the kinetics of such transitions in terms of molecular motion. A more detailed specification of geometry, rates and amplitudes of C-D bond rotations will require single-site labelling and comparison with more refined NMR line shape and nuclear relaxation simulations.

ACKNOWLEDGMENTS

This is paper number 13318 of the Agricultural Experiment Station, Purdue University. We are grateful to Kraft General Foods, Inc. for permission to publish data in this work. We acknowledge Frank Sasevich for assistance with calorimetric measurements, and David Hayashi, Robert Dinwoodie and the late Michael Kern for preparation of deuterated tripalmitins. Portions of this work were supported by the National Institutes of Health (GM-34541), an extramural grant in aid from Kraft, Inc. to R.G.B., The University of Rochester, and the Whistler Center for Carbohydrate Research, Purdue University.

REFERENCES

1. Larsson, K., *Food Microstructure 1*:55 (1982).
2. Jewell, G.G., and J.F. Heathcock, in *Food Structure: Its Creation and Evaluation*, edited by J.M.V. Blanshard, and J.R. Mitchell, Butterworths, London, 1988, p. 279.
3. Nawar, W.W., in *Food Chemistry*, edited by O. Fennema, Marcel Dekker, Inc., New York, 1985, pp. 139–244, 1985.
4. Muller, A., *Proc. Roy. Soc. Lond. A138*:514 (1932).
5. Chapman, D., in *The Structure of Lipids by Spectroscopic and X-Ray Techniques*, John Wiley & Sons, Inc., New York, 1965.
6. Small, D.M., in *Handbook of Lipid Research*, Vol. 4, Plenum Press, New York, 1986.
7. Lutton, E.S., *J. Am. Oil Chem. Soc. 27*:276 (1950).
8. Chapman, D., *Chem. Revs. 62*:433 (1962).
9. Larsson, K., *Acta Chem. Scand. 20*:2255 (1966).
10. de Jong, S., and T.C. Van Soest, *Acta Cryst. B34*:1570 (1978).
11. Govil, G., R.V. Hosur and A. Saran, *Chem. Phys. Lipids 21*:77 (1978).
12. Hosur, R.V., A. Saran and G. Govil, *Indian J. Biochem. Biophys. 16*:165 (1979).
13. Hagemann, J.W., and J.A. Rothfus, *J. Am. Oil Chem. Soc. 60*:1123 (1983).
14. Hagemann, J.W., and J.A. Rothfus, *Ibid. 60*:1308 (1983).
15. Komoroski, R.A., and L. Mandelkern, in *High Resolution NMR Spectroscopy of Synthetic Polymers in Bulk*, edited by R.A. Komoroski, VCH Publishers, Deerfield Beach, 1986.
16. Horman, I., in *Analysis of Foods and Beverages: Modern Techniques*, edited by G. Charalambous, Academic Press, Orlando, 1984, pp. 230–239.
17. Pollard, M., in *Analysis of Oils and Fats*, edited by R.J. Hamilton, and J.B. Rossell, Elsevier, New York, 1986, pp. 401–434.
18. Eads, T.M., and W.R. Croasmun, *J. Am. Oil Chem. Soc. 65*:78 (1988).
19. Eads, T.M., in *Analyses of Fats, Oils and Lipoproteins*, edited by E.G. Perkins, American Oil Chemists' Society, Champaign, 1991, pp. 409–457.
20. Chapman, D., R.E. Richards and R.W. Yorke, *J. Chem. Soc. Lond*:436 (1960).
21. Andrew, E.R., *J. Chem. Phys. 18*:607 (1950).
22. Gibon, V., F. Durant, and Cl. Deroanne, *J. Am. Oil Chem. Soc. 63*:1047 (1986).
23. Norton, I.T., C.D. Lee-Tuffnell, S. Ablett and S.M. Bociek, *Ibid. 62*:1237 (1985).
24. Azoury, R., J.S. Aronhime, S. Sarig, S. Abrashkin, I. Mayer and N. Garti, *Ibid. 6*:964 (1988).
25. Bociek, S.M., S. Ablett and I.T. Norton, *Ibid. 62*:1261 (1985).
26. Seelig, J., *Q. Rev. of Biophys. 10*:353 (1977).
27. Griffin, R.G., *Meth. Enzym. 72*:108 (1981).
28. Davis, J.H., *Biochim. Biophys. Acta 737*:117 (1983).
29. Smith, R.L., and E. Oldfield, *Science 22*:280 (1984).
30. Spiess, H.W., *Colloid and Polymer Sci. 261*:193 (1983).
31. Spiess, H.W., *Adv. Polym. Sci. 66*:23 (1985).
32. Luz, Z., *NMR in Liquid Crystals*:22 (1983).
33. Samulski, E.T., *Polymer 26*:177 (1985).
34. Gorrisen, H., A.P. Tullock and R.J. Cushley, *Chem. Phys. Lipids 31*:243 (1982).
35. Eads, T.M., A.E. Blaurock, D.J. Roy and W.R. Croasmun, paper presented at American Oil Chemists' Society Annual Meeting in Baltimore, May 1990.
36. Eads, T.M., W.R. Croasmun, A.E. Blaurock and R.G. Bryant, paper presented at American Oil Chemists' Society Annual Meeting in Cincinnati, May 1989.
37. Bryant, R.G., S.D. Kennedy, C.L. Jackson, T.M. Eads, W.R. Croasmun and A.E. Blaurock, in *NMR Applications in Biopolymers*, edited by J.W. Finley, S.J. Schmidt and A.S. Serlani, Plenum Press, New York, 1990, pp. 255–271.
38. Blaurock, A.E., *Biophys. J. 13*:290 (1973).
39. Gerstein, B.C., *Philos. Trans. R. Soc. London A299*:521 (1981).
40. Solomon, I., *Phys. Rev. 110*:61 (1958).
41. Davis, J.H., K.R. Jeffrey, M. Bloom, M.I. Valic and T.P. Higgs, *Chem. Phys. Lett. 42*:390 (1976).
42. Boden, N., and Y.K. Levine, *J. Magn. Reson. 30*:327 (1978).
43. Abragam, A., in *Principles of Nuclear Magnetism*, The Clarendon Press, Oxford, 1961.
44. deRuig, W.G., *Infrared Spectra of Monoacid Triglycerides*, Agricultural Research Report #759, from the Centre for Agricultural Publishing and Documentation, Wageningen, The Netherlands, 1971.
45. de Ruig, W.G., *Appl. Spectrosc.*:122 (1977).
46. Chapman, D., *J. Chem. Soc. Lond.*:60 (1956).
47. Chapman, D., *Ibid.*:2522 (1956).
48. Chapman, D., *Ibid*:2715 (1957).
49. Jenson, L.H., and A.J. Mabis, *Nature 197*:681 (1963).
50. Hernqvist, L., *Fat Sci. Technol. 90*:451 (1988).
51. Birker, J.M.W.L., S. de Jong, E.C. Roijers and T.C. van Soest, *J. Am. Oil Chem. Soc. 68*:895 (1991).
52. Kellens, M., W. Meeussen, C. Riekel and H. Reynaers, *Chem. Phys. Lipids 52*:79 (1990).
53. Hirschinger, J., H. Miura, K.H. Gardner and A.D. English, *Macromolecules 23*:2153 (1990).
54. Jelinski, L., and J.J. Dumais, in *Recent Advances in Analytical Methodology in the Life Sciences*, edited by L.A. Beaver, Proceedings of the 8th Food and Drug Administration Science Symposium, 1982.
55. Jelinski, L.W., J.J. Dumais and A.K. Engel, *Macromolecules 16*:492 (1983).
56. Huang, T.H., R.P. Skarjune, R.T. Wittebort, R.G. Griffin and E. Oldfield, *J. Am. Chem. Soc. 102*:7379 (1980).
57. Jeffrey, K.R., T.C. Wong and A.P. Tulloch, *Mol. Phys. 52*:289 (1984).
58. Hirschinger, J., and A.D. English, *J. Magn. Reson. 85*:542 (1989).
59. Wittebort, R.J., E.T. Olejiniczak and R.G. Griffin, *J. Chem. Phys. 86*:5411 (1987).
60. Greenfield, M.S., A.D. Ronemus, R.L. Vold and R.R. Vold, *J. Magn. Reson. 72*:89 (1987).
61. Sato, K., and T. Kuroda, *J. Am. Oil Chem. Soc. 64*:124 (1987).
62. Blaurock, A.E., F.J. Sasevich and T.M. Eads, *J. Am. Oil Chem. Soc. 65*:476 (1988).
63. Blaurock, A.E., and A.P.R. Carothers, paper presented at American Oil Chemists' Society Annual Meeting in Baltimore, May 1990.
64. Lutton, E.S., and F.L. Jackson, *J. Am. Chem. Soc. 70*:2445 (1948).
65. Jackson, F.L., and E.S. Lutton, *Ibid. 72*:4519 (1950).
66. Chapman, D., *J. Chem. Soc. Lond.*:4489 (1957).
67. Kobayashi, M., and F. Kanesho, *J. Dispersion Sci. Technol.*:319 (1989).

[Received March 24, 1992; accepted September 15, 1992]